IEEE Access
Multidisciplinary | Rapid Review | Open Access Journal

Received September 19, 2019, accepted October 3, 2019, date of publication October 10, 2019, date of current version October 25, 2019.

Digital Object Identifier 10.1109/ACCESS.2019.2946866

Fixed-Time Sliding Mode Control for Uncertain Robot Manipulators

LIYIN ZHANG, YOUMING WANG, YINLONG HOU, AND HONG LI
School of Automation, Xi'an University of Posts and Telecommunications, Xi'an 710121, China

Corresponding author: Liyin Zhang (zhangliyin@xupt.edu.cn)

This work was supported by the National Natural Science Foundation of China under Grant 51875457.

ABSTRACT This paper presents a novel fixed-time sliding mode control for the global fixed-time trajectory tracking of robot manipulators subject to uncertain dynamics and bounded external disturbances. A fixed-time sliding surface is proposed and a singularity-free fixed-time sliding mode control (SFSMC) is constructed. Lyapunov stability theory is employed to prove the global fixed-time stability ensuring that both the sliding variable and tracking errors converge globally to the origin within a fixed time. The appealing advantages of the proposed control are that it is easy to implement with the global fixed-time tracking control for uncertain robot manipulators featuring with faster transient, higher steady-state tracking precision, and the settling time is independent of the initial states of robotic system. Extensive simulations and experimental results are presented to demonstrate the effectiveness and improved performances of the proposed approach.

INDEX TERMS Robot manipulators, sliding mode control, robust control, fixed-time stability, single inverted pendulum.

I. INTRODUCTION

During the past decades, many significant research efforts [1]–[9] have been devoted to investigating the trajectory tracking of robot manipulators subject to uncertain dynamics and bounded external disturbances. Among them, sliding mode controls (SMC) [1]–[4] featuring with the insensitivity property to uncertain dynamics and bounded external disturbances is a powerful method to control uncertain robot manipulators. The formulation of SMC consists mainly of two steps, i.e., the choice of the sliding surface and sliding mode controller. The sliding surface is chosen such that an SMC system can behave in a desirable fashion and then the proposed controller is designed to guarantee that the system can be driven to reach the sliding surface and remain on it for further time. Since its fast convergence, simplicity of implementation, order reduction, high robustness to external disturbances and insensitivity to uncertain dynamics and system parameter variations, SMC has widely been used for the trajectory tracking of robot manipulators with uncertain dynamics and bounded external disturbances.

Terminal sliding mode control (TSMC) [10] is an easy-going solution for robust finite-time stable tracking of uncertain robot manipulators, which guarantees that both the sliding variable and tracking errors converge globally to the origin within a finite time. Based on this seminal work, two TSMCs [1], [2] are developed for the trajectory tracking of uncertain robot manipulators. However, these TSMCs suffer from a fatal drawback, i.e., the singularity problem [11]. Then, several different non-singular TSMCs [3], [4], [12]–[15] have been developed to overcome the singularity of the TSMC schemes. Among them, the TSMCs [3], [4], [12] require the upper bound of the lumped uncertainty involving the joint acceleration; while the approaches [14], [15] directly use the joint acceleration in the control law formulation. Accordingly, these non-singular TSMCs are not easily adopted for the practical application owing to the usage of joint acceleration [16], [17]. The methods [18], [19] to avoid the singularity are presented by introducing some rigorous constraints on the sliding surface. Another method [20] to avoid the singularity is proposed by transforming the nonlinear sliding surface to a linear one. Zhang et al. [21] investigates a continuous sliding mode control for uncertain robot manipulators. A chattering-free integral sliding mode control scheme is proposed by integrating an integral sliding surface with an observer. Since both the sliding variable and tracking errors converge globally to the origin within a finite time, the mentioned SMCs have been

The associate editor coordinating the review of this manuscript and approving it for publication was Yangmin Li.

considered as the finite-time sliding mode controls and thus its convergence time depends on the initial states of robotic system.

The main weakness of these finite-time sliding mode controls is that the settling time depends on the initial states of closed-loop system. It infers that the settling time of trajectory tracking cannot acquired in advance. Recently, a further development of the finite-time control named as fixed-time control has been developed. In comparison with the finite-time stable control, the fixed-time stable control guarantees that the settling time is uniformly bounded by a fixed time and independent of initial states. More specifically, the approaches [22]–[25] give a detailed survey on the mathematical tools for the fixed-time stability and convergence analysis of controlled systems. Tian et al. [26] proposes a continuous output feedback control scheme for the fixed-time stabilization of the double integrator system, where the bi-limit homogeneous technique is used for controller and observer design and analysis. A predefined-time control [27] is developed for a class of nonlinear dynamical systems for which the minimum bound of the settling-time function can be obtained as an explicit parameter of the system in advance. Zuo [28] proposes a TSMC for fixed-time stabilization of double integrators and applies for consensus tracking of second-order multi-agent systems. This fixed-time stable control is later extended for a class of nonlinear second-order systems in the form of double integrators with matched uncertainties and perturbations [29]. A novel fixed-time sliding mode control [30] is developed for the single inverted pendulum (SIP) system. The above literature review reveals that the most existing fixed-time stable controls are developed for linear and nonlinear affine systems and cannot easily be used for multi-DOFs uncertain robot manipulators.

In this paper, a novel singularity-free fixed-time sliding mode control (SFSMC) is proposed for the trajectory tracking of robot manipulators in the presence of uncertain dynamics and bounded external disturbances. The contributions of our paper are as follows: (i) The proposed SFSMC is constructed without using the acceleration of joints or the assumption that the lumped uncertainty involving the acceleration of joints are bounded by a constant, which not only overcomes the singularity of commonly used TSMCs but also obtain the fixed-time tracking of uncertain robot manipulators; (ii) In comparison with the existing finite-time sliding mode controls [3], [4], [12], [21], the convergence time of the proposed SFSMC is independent of the initial states of robotic system and can be acquired in advance; (iii) In comparison with the similar fixed-time control for dynamical system presented by [28]–[30], the main contributions of this novel sliding surface design are twofold. It is clear from Zuo [28] and Li [30] that the non-singular fixed-time controls are originally proposed for single-input-single-out systems and both of them require the exact control gain matrix. Hence, they are not directly applicable to multi-DOFs uncertain robot manipulators due to it involves the unknown inertia matrix and the dynamical coupling between multi-joints. Lyapunov stability theory is employed to prove the global fixed-time stability ensuring that both the sliding variable and tracking errors converge globally to the origin within a fixed time. Simulation comparisons with the fast TSMC (FTSMC) [12] and the integral terminal sliding mode control (ITSMC) [21] have been performed for uncertain robot manipulators. To further show the improved tracking performance compared with the fixed-time sliding mode controls [29], [30], thereafter, extensive simulations and experimental results have been accomplished for the single inverted pendulum (SIP) system and the one-DOF mechanical system, respectively. The simulation and experimental results demonstrate that the proposed controller gains the performance improvement including faster transient and higher steady-state tracking precision for trajectory tracking of uncertain robot manipulators.

Throughout this paper, we use the notation $\lambda_{\min}\{A\}$ and $\lambda_{\max}\{A\}$ to indicate the smallest and largest eigenvalues, respectively, of a symmetric positive definite matrix A. For any $x \in R^n$, the norm of vector x is defined as $\|x\| = x^T x$ and that of matrix A is defined as the corresponding induced norm $\|A\| = \lambda_{\max}\{A^T A\}$.

The reminder of this paper is organized as follows. In Section 2, some preliminaries including the model and properties of robot manipulators and fixed-time stability of dynamical systems are introduced. The controller design and stability analysis are presented in Section 3. In Sections 4 and 5, numerical comparisons are performed. Finally, a conclusion is included in Section 6.

II. PRELIMINARIES

A. ROBOT MANIPULATOR MODEL AND PROPERTIES

The n-joint rigid manipulators are described as [31]

$$M(q)\ddot{q} + C(q,\dot{q})\dot{q} + g(q) = \tau + d \tag{1}$$

where $q,\ \dot{q},\ \ddot{q} \in R^n$ denote the vectors of position, velocity and acceleration, respectively, $M(q) \in R^{n\times n}$ is the symmetric positive definite inertia matrix, $C(q,\dot{q}) \in R^{n\times n}$ stands for the centrifugal-Coriolis matrix, $g(q) \in R^n$ denotes the vector of gravitational torque, $d \in R^n$ denotes the bounded external disturbances and is upper bounded by $\|d\| \le d_M$ with a known constant d_M, and $\tau \in R^n$ is the control input.

Our design will be accomplished on the following fundamental facts [3], [31].

Property 1: The matrices $M(q)$ and $C(q,\dot{q})$ and the vector $g(q)$ are upper bounded by [31]

$$\begin{aligned} \|M(q)\| &\le M_M \\ \|C(q,\dot{q})\| &\le C_M\,\|\dot{q}\| \\ \|g(q)\| &\le G_M \end{aligned} \tag{2}$$

where M_M, C_M and G_M are some known positive constants.

The subsequent development is based on the assumption that q is available, $\dot{q}$ can be estimated by using the joint position q properly, and the desired trajectory $q_d \in R^n$ be C^2 for the robotic system. Additionally, the following assumption will be exploited [3].

Assumption 1: The model parameters can be described as

$$\begin{aligned} M(q) &= M_0(q) + \Delta M(q) \\ C(q,\dot{q}) &= C_0(q,\dot{q}) + \Delta C(q,\dot{q}) \\ g(q) &= g_0(q) + \Delta g(q) \end{aligned} \tag{3}$$

where $M_0(q)$, $C_0(q,\dot{q})$ and $g_0(q)$ denote the nominal parts, and $\Delta M(q)$, $\Delta C(q,\dot{q})$ and $\Delta g(q)$ stand for the uncertain parts.

According to Property 1 and (3), the following property can be obtained.

Property 2: The matrices $\Delta M(q)$ and $\Delta C(q,\dot{q})$ and the vector $\Delta g(q)$ are upper bounded by

$$\begin{aligned} \|\Delta M(q)\| &\le M_m \\ \|\Delta C(q,\dot{q})\| &\le C_m \|\dot{q}\| \\ \|\Delta g(q)\| &\le G_m \end{aligned} \tag{4}$$

where M_m, C_m and G_m are some known positive constants.

Without loss of generality, it is assumed that the norms of desired vectors are upper bounded by

$$\|q_d\| \le P_p, \quad \|\dot{q}_d\| \le P_v, \quad \|\ddot{q}_d\| \le P_a \tag{5}$$

where q_d, $\dot{q}_d$, $\ddot{q}_d \in R^n$ are the vector of desired position, velocity and acceleration, respectively, and P_p, P_v and P_a are some known positive constants.

To facilitate the following design and analysis, we define the vector $\mathrm{Sig}^r(\xi) \in R^n$ and the matrix $\mathrm{D}^r(\xi) \in R^{n\times n}$ as

$$\mathrm{Sig}^r(\xi) = \left[\mathrm{sig}^r(\xi_1),\ \ldots,\ \mathrm{sig}^r(\xi_n)\right]^T \tag{6}$$

$$\mathrm{D}^r(\xi) = \mathrm{diag}\{|\xi_i|^r\}, \quad i = 1,\ldots,n \tag{7}$$

where $\mathrm{diag}\{\cdot\}$ denotes the diagonal matrix, ξ_i is the ith component of the vector $\xi \in R^n$, r is a positive constant and $\mathrm{sig}^r(\xi_i)$ is a continuous function and defined as

$$\mathrm{sig}^r(\xi_i) = |\xi_i|^r \mathrm{sign}(\xi_i), \quad i = 1,\ \ldots,\ n \tag{8}$$

with $\mathrm{sign}(\cdot)$ denotes the standard signum function.

The objective of this paper is to design a novel singularity-free fixed-time sliding mode control (SFSMC) for robot manipulators subject to the uncertain dynamics and bounded external disturbances such that both the sliding variable and tracking errors converge globally to the origin within a pre-defined time.

To quantify this objective, the definition of the position and velocity tracking errors are defined as follows

$$e = q - q_d, \quad \dot{e} = \dot{q} - \dot{q}_d \tag{9}$$

B. FUNDAMENTAL FACTS

Definition 1(Fixed-Time Stability) [23]: Consider the system $\dot{x} = g(t,x)$ with $x(0) = x_0$, where $x \in R^n$ and $g : R^+ \times R^n \to R^n$ is a nonlinear function which can be discontinuous. The origin of the system $\dot{x} = g(t,x)$ is said to be globally fixed-time stable if the settling time function T is globally bounded, i.e., there exists a fixed constant $T_{\max} \in R^+$ such that $T \le T_{\max}$ and $x(t) = 0$ for all $t \ge T$ and $x_0 \in R^n$.

Lemma 1: Consider a scalar system [28], [32]

$$\dot{y} = -\alpha \mathrm{sig}^{\frac{m}{n}}(y) - \beta \mathrm{sig}^{\frac{p}{k}}(y), \quad y(0) = y_0 \tag{10}$$

where m, n, p and k are all positive *odd* integers satisfying $m > n$ and $p < k$, $\alpha > 0$ and $\beta > 0$ and $\mathrm{sig}^{\frac{m}{n}}(y)$ and $\mathrm{sig}^{\frac{p}{k}}(y)$ are defined by (8). Then, the equilibrium point of the system (10) is fixed-time stable, and the settling time T is bounded by

$$T < T_{\max} \triangleq \frac{1}{\alpha}\frac{n}{m-n} + \frac{1}{\beta}\frac{p}{k-p} \tag{11}$$

Proof [32]: Let $V(y) = y^2 \ge 0$. Differentiating $V(y)$ along with system (10) yields

$$\begin{aligned} \dot{V} &= 2y\left(-\alpha \mathrm{sig}^{\frac{m}{n}}(y) - \beta \mathrm{sig}^{\frac{p}{k}}(y)\right) \\ &= -2\alpha (y^2)^{\frac{m+n}{2n}} - 2\beta (y^2)^{\frac{p+k}{2k}} \\ &= -2\left(\alpha V^{\frac{m+n}{2n}-\frac{p+k}{2k}} + \beta\right) V^{\frac{p+k}{2k}} \end{aligned} \tag{12}$$

The fact $\alpha V^{(m+n)/2n-(p+k)/2k} > 0$ implies that $\dot{V}(y) \le -2\beta V^{(p+k)/2k}$. In light of $0 < \frac{p+k}{2k} < 1$, the system (10) is globally finite-time stable due to Lemma 3.2 of [32]. Then, since $V(y) = 0$ from (12) is a trivial case, assuming $V(y) \ne 0$, we have

$$\begin{aligned} \frac{1}{V^{\frac{p+k}{2k}}}\frac{dV}{dt} &= -2\left(\alpha V^{\frac{m+n}{2n}-\frac{p+k}{2k}} + \beta\right) \\ \Rightarrow \frac{2k}{k-p}\frac{dV^{\frac{k-p}{2k}}}{dt} &= -2\left(\alpha V^{\frac{m+n}{2n}-\frac{p+k}{2k}} + \beta\right) \end{aligned} \tag{13}$$

Let $z = V^{(k-p)/2k}$. (13) can be written as

$$\frac{1}{\alpha z^{1+\varepsilon} + \beta}\mathrm{d}z = -\frac{k-p}{k}\mathrm{d}t \tag{14}$$

where $\varepsilon \triangleq \frac{k(m-n)}{n(k-p)}$. Let $\varphi(z) = \int_0^z \frac{1}{\alpha z^{1+\varepsilon}+\beta}\mathrm{d}z$, integrating both sides of the preceding equation yields

$$\varphi(z(t)) = \varphi(z(0)) - \frac{k-q}{k}t \tag{15}$$

Since the function $\varphi(z(t))$ is monotonically increasing, $\varphi(z(t)) = 0$ if and only if $z = 0$, which implies $V = 0$. Thus we have

$$\lim_{t\to T(y_0)} V = 0 \tag{16}$$

where $T(y_0)$ denotes the settling time function given by

$$T(y_0) = \frac{k}{k-p}\varphi(z(0)) = \frac{k}{k-p}\varphi(y^{(k-p)/k}(0)) \tag{17}$$

Toward this end, it can be verified that $T(y_0)$ is bounded by

$$\begin{aligned} &\lim_{y_0\to\infty} T(y_0) \\ &= \lim_{z_0\to\infty}\frac{k}{k-p}\varphi(z(0)) = \frac{k}{k-p}\varphi(\infty) \\ &= \frac{k}{k-p}\left(\int_0^1 \frac{1}{\alpha z^{1+\varepsilon}+\beta}\mathrm{d}z + \int_1^\infty \frac{1}{\alpha z^{1+\varepsilon}+\beta}\mathrm{d}z\right) \\ &< \frac{k}{k-p}\left(\int_0^1 \frac{1}{\beta}\mathrm{d}z + \int_1^\infty \frac{1}{\alpha z^{1+\varepsilon}}\mathrm{d}z\right) \\ &= \frac{k}{k-p}\left(\frac{1}{\beta} + \alpha\varepsilon\right) = \frac{1}{\alpha}\frac{n}{m-n} + \frac{1}{\beta}\frac{k}{k-p} \end{aligned} \tag{18}$$

Using the fact that $V(y(t)) = 0$ implies $y(t) = 0$ completes the proof of Lemma 1.

Lemma 2: For $0 < \kappa < 1$, the following inequality holds [28]

$$\sum_{i=1}^{n} |x_i|^{1+\kappa} \geq \left(\sum_{i=1}^{n} |x_i|^2 \right)^{\frac{1+\kappa}{2}} \tag{19}$$

Lemma 3: For $\kappa > 1$, the following inequality holds [28]

$$\sum_{i=1}^{n} |x_i|^{\kappa} \geq n^{1-\kappa} \left(\sum_{i=1}^{n} |x_i| \right)^{\kappa} \tag{20}$$

III. CONTROL DESIGN AND STABILITY ANALYSIS

To facilitate the subsequent control design and stability analysis, we begin with the open-loop error system development aimed to obtain an upper bound of the lumped uncertainty that does not involve the joint acceleration. Thereafter, the control formulation presents the fixed-time sliding surface and fixed-time stable control law, along with fixed-time stability analysis.

A. OPEN-LOOP SYSTEM DEVELOPMENT

Based on Assumption 1, the system (1) can be rewritten as

$$M_0(q)\ddot{q} + C_0(q,\ \dot{q})\dot{q} + g_0(q) = \tau + \rho \tag{21}$$

where the lumped uncertainty $\rho \in R^n$ is defined as

$$\rho = -\Delta M(q)\ddot{q} - \Delta C(q,\ \dot{q})\dot{q} - \Delta g(q) + d \tag{22}$$

In light of (1) and (3), it follows that

$$\Delta M(q)\ddot{q} = E(\tau - C(q,\ \dot{q})\dot{q} - g(q) + d) \tag{23}$$

where $E \in R^{n\times n}$ defined by [16]

$$E = I_n - M_0(q)M^{-1}(q) \tag{24}$$

and I_n denotes the $n \times n$ identity matrix.

Observed by the work, once $M_0(q)$ is chosen as [16]

$$M_0 = \frac{2}{\gamma_1 + \gamma_2} I_n \tag{25}$$

where γ_1 and γ_1 are two known positive constants defined by

$$\gamma_1 \leq \left\| M^{-1}(q) \right\| \leq \gamma_2 \tag{26}$$

then E is upper bounded by [16]

$$\|E\| \leq \sigma \tag{27}$$

with σ stands for a known positive constant given by

$$\sigma = \frac{\gamma_2 - \gamma_1}{\gamma_1 + \gamma_2} \tag{28}$$

Note that $M_0(q)$ is written as M_0 in the subsequent development owing to the $M_0(q)$ defined by (25) is a constant matrix.

By virtue of Properties 1 and 2, Assumption 1, (23) and (27), the lumped uncertainty ρ given by (22) is upper bounded by [16]

$$\|\rho\| \leq a_0 + a_1\|\dot{q}\|^2 + \sigma\ \|\tau\| \tag{29}$$

where σ is defined by (28) and $a_i,\ i = 0, 1$ denote two positive constants that depend on the robotic system.

B. CONTROL FORMULATION

Firstly, a nonlinear function $f(x)$ is proposed as follows [33]

$$f(x) = \begin{cases} K_a \mathrm{sig}^r(x) + K_b \delta^{|x|} x, & \text{if } |x| < \delta \\ \mathrm{sig}^{\alpha}(x), & \text{if } |x| \geq \delta \end{cases} \tag{30}$$

where x denotes the variable, $r = \alpha + 1$, α and δ are some positive constants with $\alpha = 1 - \delta$, $\delta \in (0,\ \exp(-1))$, $\mathrm{sig}^r(x)$ and $\mathrm{sig}^{\alpha}(x)$ are the continuous function and defined by (8) and

$$K_a = \frac{-1 - \ln \delta}{\alpha - \delta \ln \delta}, \quad K_b = \frac{\delta^{2\alpha-2}}{\alpha - \delta \ln \delta} \tag{31}$$

The first derivative of $f(x)$ with respect to x is

$$h(x) = \begin{cases} K_a r|x|^{r-1} + K_b(\,|x| \ln\delta + 1)\delta^{|x|}, & \text{if } |x| < \delta \\ \alpha |x|^{\alpha-1}, & \text{if } |x| \geq \delta \end{cases} \tag{32}$$

Note that the choice of K_a and K_b guarantees that the function $f(x)$ and its derivative $h(x)$ are continuous when $|x| = \delta$. $f(x)$ and $h(x)$ are bounded by $k_f\,|x|$ and k_h, respectively, where these two positive constants k_f and k_h are defined as [33]

$$\begin{aligned} k_f &= \frac{\delta^{2\alpha-2} - 1 - \ln \delta}{\alpha - \delta \ln \delta} \\ k_h &= \frac{\delta^{\alpha}(\delta^{\alpha-2} - r) - (r + \delta^{\alpha-1})\delta^{\alpha} \ln \delta}{\alpha - \delta \ln \delta} \end{aligned} \tag{33}$$

The proof of the upper bounds of $f(x)$ and $h(x)$ can be found in [33]. Figure 1 gives an illustration of $f(x)$ and $h(x)$ with their bounds for $\delta = 0.2$ and $\alpha = 1 - \delta$. Observed by Figure 1, clearly, $f(x)$ and $h(x)$ are continuous function and upper bounded by $k_f|x|$ and $h(x)$, respectively.

To facilitate the subsequent design and analysis, the vector $F(e) \in R^n$ and the diagonal matrix $B(e) \in R^{n\times n}$ are defined as follows

$$F(e) = [f(e_1), f(e_2), \ldots\ldots, f(e_n)]^T \tag{34}$$

$$B(e) = \mathrm{diag}\,\{h(e_i)\}, \quad i = 1, 2, \ldots, n \tag{35}$$

where e_i is the ith component of the vector e given by (9), and $f(e_i)$ and $h(e_i)$ are described by (30) and (32), respectively.

Based on the above nonlinear function, a vector of singularity-free fixed-time sliding surface is designed as

$$S = \dot{e} + C_1 F(e) + C_2 \mathrm{Sig}^{\beta}(e) \tag{36}$$

where $C_1,\ C_2 \in R^{n\times n}$ are two positive definite diagonal matrixes, $\beta > 1$ denotes a known positive constant, and $\mathrm{Sig}^{\beta}(\cdot)$ and $F(e)$ are defined by (6) and (34), respectively.

Upon differentiating S with respect to time, we have

$$\dot{S} = \ddot{e} + C_1 B(e)\dot{e} + C_2 \mathrm{D}^{\beta-1}(e)\dot{e} \tag{37}$$

where $\mathrm{D}^{\beta-1}(\cdot)$ and $B(e)$ are defined by (7) and (35), respectively.

After substituting (9) and (37) into (21), the error closed-dynamic equation for S takes

$$M_0\dot{S} = \tau + \rho + \eta \tag{38}$$

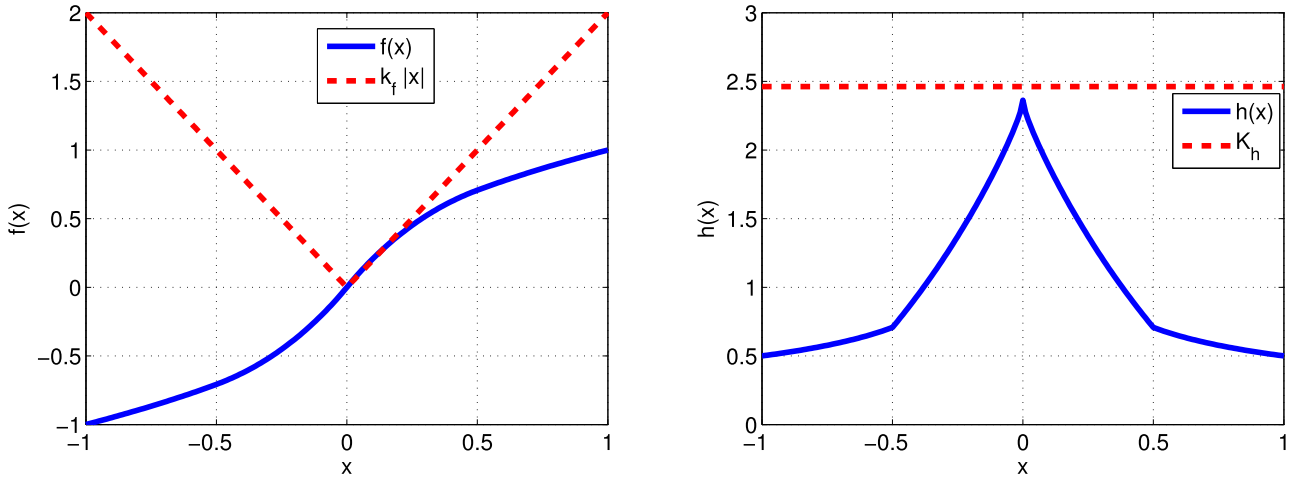

(a) $f(x)$ and its bounds. (b) $h(x)$ and its bounds.

FIGURE 1. *f(x) and h(x) with their bounds.*

where the lumped uncertainty $\rho \in R^n$ is defined by (22) and the nominal part $\eta \in R^n$ is described as follows

$$\eta = C_1 M_0 B(e)\dot{e} + C_2 M_0 \mathrm{D}^{\beta-1}(e)\dot{e} - C_0(q,\ \dot{q})\dot{q} - g_0(q) - M_0\ddot{q}_d \quad (39)$$

For system (38), the first step to accomplish our objective is to design a fixed-time sliding mode control subject to uncertain dynamics and bounded external disturbances such that the sliding variable (36) converges to the origin (i.e. $S = 0$) within a fixed time. Then, the singularity-free fixed-time sliding mode control (SFSMC) is defined as

$$\tau = -\eta + \tau_0 + \tau_1 \quad (40)$$

where $\eta \in R^n$ is defined by (39) and

$$\tau_0 = -K_1 \mathrm{Sig}^{\nu_1}(S) - K_2 \mathrm{Sig}^{\nu_2}(S) \quad (41)$$

$$\tau_1 = -b(S)w \quad (42)$$

with

$$b(S) = \begin{cases} \dfrac{S}{\|S\|}, & \|S\| \neq 0 \\ 0, & \|S\| = 0 \end{cases} \quad (43)$$

$$w = \frac{1}{1-\sigma}\left(a_0 + a_1\|\dot{q}\|^2 + \sigma\,\|\tau_0 - \eta\|\right) \quad (44)$$

where $K_1,\ K_2 \in R^{n\times n}$ denote two positive definite diagonal matrixes, $\nu_1 > 1$ and $0 < \nu_2 < 1$ are some positive constants, and σ, a_0 and a_1 are defined by (28) and (29), respectively.

After substituting (40) into (38), we have

$$M_0\dot{S} = \tau_0 + \tau_1 + \rho \quad (45)$$

C. STABILITY ANALYSIS

For system (45), we are in a position to state the following result.

Theorem 1: Given the uncertain robot manipulators for S given by (45), firstly, the proposed SFSMC defined by (40)-(44) ensures that the tracking trajectory converges globally to the fixed-time sliding surface (36) ($S = 0$) within a fixed time T_r. Then, the tracking errors along with the fixed-time sliding surface (36) converge to an arbitrary small domain of the origin $B_\delta = \{e_i\,||e_i| \le \delta\}$ within a fixed time T_s, and thereafter arrive at the origin asymptotically. Then, the convergence time independent of the initial states is guaranteed for the uncertain robot manipulators. The settling time is derived as

$$T < T_{\max} \triangleq T_r + T_s \quad (46)$$

where T_r and T_s denote the reaching and sliding time, respectively. They are defined as

$$T_r \le \frac{2}{\lambda_{\min}\{K_1\}n^{(1-\nu_1)/2}(\nu_1 - 1)} + \frac{2}{\lambda_{\min}\{K_2\}(1-\nu_2)} \quad (47)$$

$$T_s \le \frac{2}{c_{1i}(1-\alpha)} + \frac{2}{c_{2i}(\beta - 1)} \quad (48)$$

Proof: To aid subsequent proof, the stability analysis of the proposed SFSMC can be divided into the following two steps, i.e., the stability analysis in reaching phase and sliding phase.

Step 1 Stability Analysis in Reaching Phase:

In reaching phase, for system (45), the objective of this step is to prove that the sliding surface defined by (36) converges globally to the origin within a fixed time T_r given by (47). Firstly, the positive definite Lyapunov function candidate for system (45) is proposed as follows

$$V = \frac{1}{2}S^T M_0 S \quad (49)$$

Note that M_0 is a constant matrix from (25) and then differentiating V with respect to time along the trajectory of dynamics equation (45), we have

$$\dot{V} = S^T M_0 \dot{S} \quad (50)$$

After substituting (45) for $M_0\dot{S}$ into (50) yields

$$\dot{V} = S^T(\tau_0 + \tau_1 + \rho) \tag{51}$$

Then, substituting (40)-(44) into (51), we have obtained

$$\begin{aligned}\dot{V} &= -S^T(K_1\mathrm{Sig}^{\nu_1}(S) + K_2\mathrm{Sig}^{\nu_2}(S)) - w\|S\| + S^T\rho \\ &\leq -S^T(K_1\mathrm{Sig}^{\nu_1}(S)+K_2\mathrm{Sig}^{\nu_2}(S)) - w\|S\| + \|\rho\|\|S\| \end{aligned} \tag{52}$$

By utilizing the upper bound of ρ defined by (29), it follows that

$$\begin{aligned}\dot{V} &\leq -w\|S\| + (a_0 + a_1\|\dot{q}\|^2 + \sigma\|\tau\|)\|S\| \\ &\quad -S^T(K_1\mathrm{Sig}^{\nu_1}(S) + K_2\mathrm{Sig}^{\nu_2}(S)) \\ &\leq -w\|S\| + (a_0 + a_1\|\dot{q}\|^2 + \sigma\|\tau_0 - \eta\|)\|S\| \\ &\quad +\sigma\|\tau_1\|\|S\| \ - S^T(K_1\mathrm{Sig}^{\nu_1}(S) + K_2\mathrm{Sig}^{\nu_2}(S)) \end{aligned} \tag{53}$$

where the fact $\|\tau\| \leq \|\tau_0 - \eta\| + \|\tau_1\|$ is used from (40).

In light of (44), we have obtained

$$\begin{aligned}&-w\|S\| + (a_0 + a_1\|\dot{q}\|^2 + \sigma\|\tau_0 - \eta\|)\|S\| + \sigma\|\tau_1\|\|S\| \\ &\quad = -(1-\sigma)w\|S\| - \sigma w\|S\| + \sigma\|\tau_1\|\|S\| \\ &\qquad +(a_0 + a_1\|\dot{q}\|^2 + \sigma\|\tau_0 - \eta\|)\|S\| \\ &\quad = -\sigma w\|S\| + \sigma\|\tau_1\|\|S\| \\ &\quad = 0 \end{aligned} \tag{54}$$

Note that in the derivation of (54) the fact that $\|\tau_1\| = w$ with $w > 0$ is involved from (42) and (44).

Upon substituting (54) into (53), we have

$$\dot{V} \leq -S^T K_1\mathrm{Sig}^{\nu_1}(S) - S^T K_2\mathrm{Sig}^{\nu_2}(S) \tag{55}$$

By Lemmas 2 and 3 and the facts of $\nu_1 > 1$ and $0 < \nu_2 < 1$, we have

$$\begin{aligned}S^T K_1\mathrm{Sig}^{\nu_1}(S) &\geq \lambda_{\min}\{K_1\}\sum_{i=1}^{n}|S_i|^{1+\nu_1} \\ &\geq \lambda_{\min}\{K_1\}n^{\frac{1-\nu_1}{2}}\left(\sum_{i=1}^{n}|S_i|^2\right)^{\frac{1+\nu_1}{2}} \end{aligned} \tag{56}$$

$$\begin{aligned}S^T K_1\mathrm{Sig}^{\nu_2}(S) &\geq \lambda_{\min}\{K_2\}\sum_{i=1}^{n}|S_i|^{1+\nu_2} \\ &\geq \lambda_{\min}\{K_2\}\left(\sum_{i=1}^{n}|S_i|^2\right)^{\frac{1+\nu_2}{2}} \end{aligned} \tag{57}$$

Upon utilising (56), (57) and the fact $lV = \|S\|^2$ with $l = \gamma_1 + \gamma_2$ from (25) and (49) to (55), we have

$$\dot{V} \leq -\lambda_{\min}\{K_1\}n^{\frac{1-\nu_1}{2}}(V)^{\frac{1+\nu_1}{2}} - \lambda_{\min}\{K_2\}(V)^{\frac{1+\nu_2}{2}} \tag{58}$$

Obviously, if $V \neq 0$, then let $y = V$ be the solution to the differential equation (10). Accordingly, it follows from Lemma 1 and 'Comparison Principle' of differential equations [34] that the tracking trajectory will reach the sliding surface (i.e. $S = 0$) within a fixed time T_r defined by (47). Note that $V = 0$ implies $S = 0$ from (36) and (49).

Step 2 Stability Analysis in Sliding Phase:

In sliding phase, the objective of this step is to prove that the position tracking errors along with the sliding surface (36) converges globally to the origin.

Once $S = 0$ (i.e. $S = \dot{e} + C_1F(e) + C_2\mathrm{Sig}^{\beta}(e) = 0$ according to (36)), the trajectory of robot manipulators enters the sliding phase from the reaching phase. According to (30) and (36), the convergence of tracking errors on sliding phase can be decomposed into the following two cases.

Case a: When $|e_i(T_r)| \geq \delta$, according to (30), (34) and (36), the dynamics of e_i are

$$\dot{e}_i = -c_{1i}\mathrm{sig}^{\alpha}(e_i) - c_{2i}\mathrm{sig}^{\beta}(e_i), \quad i = 1, \ldots, n \tag{59}$$

Obviously, then let $y = e_i$ be the solution to the differential equation (10). Accordingly, it follows from Lemma 1 and 'Comparison Principle' of differential equations [34] that the tracking error e_i converges to an arbitrary small domain of the origin $B_\delta = \{e_i \,||e_i| \leq \delta\}$ within a fixed time T_s given by (48).

Case b: When $|e_i(T_r)| < \delta$, similarly, the dynamics of e_i are

$$\dot{e}_i = -c_{1i}\left(K_a\mathrm{sig}^{r}(e_i) + K_b\delta^{|e_i|}e_i\right) - c_{2i}\mathrm{sig}^{\beta}(e_i), \quad i = 1, \ldots, n \tag{60}$$

For system (60), the positive definite Lyapunov function candidate is proposed as

$$V_1 = \frac{1}{2}e_i^2 \tag{61}$$

Differentiating V_1 with respect to time along with the system (60), we have

$$\begin{aligned}\dot{V}_1 &= e_i\dot{e}_i \\ &= -c_{1i}K_a|e_i|^{r+1} - c_{1i}K_b\delta^{|e_i|}e_i^2 - c_{2i}|e_i|^{\beta+1} \end{aligned} \tag{62}$$

Based on the facts of $K_a > 0$ and $K_b > 0$ with $\delta \in (0, \ \exp(-1))$, we can obtain the result $\dot{V}_1 < 0$. On the fundamental of Lyapunov theorem, the states of the system (60) converge globally to the origin asymptotically.

According to the stability analysis of ***Cases a*** and ***b***, we can obtain the fact that the position error $e_i(t)$ of robotic system converges globally to an arbitrary small domain of the origin $B_\delta = \{e_i \,||e_i| \leq \delta\}$ within a fixed time T_s given by (48) and thereafter arrives at the origin asymptotically. This completes the stability analysis in sliding phase.

Accordingly, in light of the discussion of **Steps 1** and **2**, we can conclude that the tracking trajectory converges firstly to the sliding surface (36) within a fixed time T_r given by (47). Once $S = 0$, the tracking error $e_i(t)$ along with the proposed fixed-time sliding surface converges globally to an arbitrary small domain of the origin $B_\delta = \{e_i \,||e_i| \leq \delta\}$ within a fixed time T_s given by (48) and thereafter arrives at the origin asymptotically. This completes the proof.

Remark 1: The proposed SFSMC does not refer to model parameters in the control law formulation and would gain global fixed-time tracking of robot manipulators in the presence of uncertain dynamics and bounded external disturbances. Compared with the existing finite-time

TSMCs [2]–[4], the settling time of the proposed approach is independent of the initial states and can be calculated in advance. Moreover, the proposed SFSMC removes the algebraic loop problem [16] existed in the TSMCs for uncertain robot manipulators [2]–[4].

Remark 2: It is important to note that the non-singular sliding surfaces for fixed-time convergence has been proposed by Zuo [29] and Li and Cai [30]. Compared with the non-singular fixed-time sliding mode control (NFSMC) of Zuo [29] and the fast fixed-time sliding mode control (FFSMC) of Li and Cai [30], the proposed singularity-free fixed-time sliding mode cntrol (SFSMC) uses the freely chosen power constants satisfying $1 < r < 2$ and $0 < \alpha < 1$; while the NFSMC of Zuo [29] requires odd integers satisfying $m_1 > n_1$, $p_1 < q_1 < 2p_1$, and $m_1/n_1 - p_1/q_1 > 1$, and the FFSMC of Li and Cai [30] couples the proportional gain and power gains together, and hence the proposed SFSMC has a large possibility to give a faster convergence over the NFSMC of Zuo [29] and FFSMC of Li and Cai [30]. The proposed SFSMC has a simple structure and it is easy to implement with multi-DOFs robotic systems. Moreover, a novel nonlinear function (30) is applied in the proposed sliding surface (36). As a consequence, a faster convergence of the proposed sliding surface (36) ($S = 0$) is expected.

Now let us illustrate the claim of Remark 2 with one-DOF case by using the convergence comparisons of the NFSMC, FFSMC and the proposed SFSMC in sliding phase. The sliding surface of the NFSMC is [29]

$$S = e + \text{sig}^{q_1/p_1}(\kappa \dot{e}) \tag{63}$$

with

$$\kappa(e) = \frac{1}{a_1|e|^{m_1/n_1 - p_1/q_1} + c_1} > 0 \tag{64}$$

where m_1, n_1, q_1 and p_1 are odd integers satisfying $m_1 > n_1$, $p_1 < q_1 < 2p_1$ and $m_1/n_1 - p_1/q_1 > 1$, and a_1 and c_1 denote some positive constants.

While the sliding surface of FFSMC is [30]

$$S = \text{sig}^{a_1}(e) + \frac{k_2 a_2}{2a_2 - 1}\text{sig}^{2-1/a_2}(\dot{e} + k_1 \text{sig}^{a_1}(e)) \tag{65}$$

where $k_1 > 0$, $k_2 > 0$, $a_2 > 1$ and $1 < a_1 < 2 - 1/a_2$.

The same initial state $e(0) = 0.5$. The parameters of the proposed SFSMC are chosen as $\alpha = 0.7$, $\delta = 0.3$, $r = 1.7$ and $\beta = 1.1$; while the parameters of the NFSMC are chosen as $a_1 = c_1 = 1$, $m_1/n_1 = 2.5$ and $q_1/p_1 = 1.5$, and that of the FFSMC [30] are $k_1 = k_2 = 1$, $a_1 = 1.1$ and $a_2 = 1.5$. The convergence of these three sliding surfaces are illustrated in Figure 2. It can be seen from Figure 2 that the proposed sliding surface given by (36) has faster convergence than the sliding surface of the NFSMC and FFSMC defined by (63) and (65) in sliding phase, respectively.

Remark 3: To reduce the undesired chattering of the proposed SFSMC, the following boundary layer method is used to replace the discontinuous control of (42). That is [30]

$$\tau_1 = -\psi(\rho_w,\ S)w \tag{66}$$

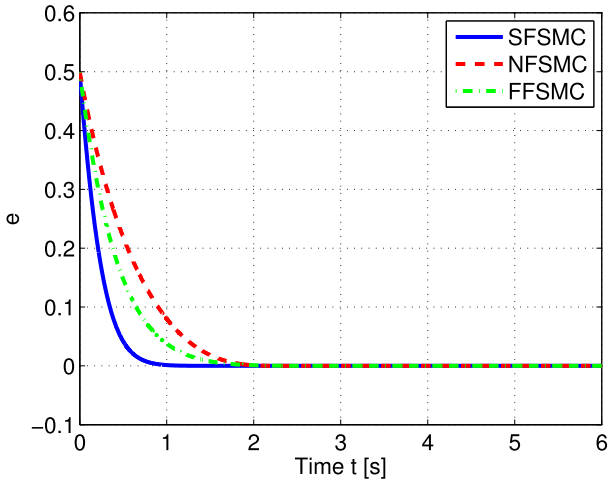

FIGURE 2. Comparison among the sliding surfaces of SFSMC, FFSMC and NFSMC.

with

$$\psi(\rho_w,\ S) = \frac{\exp(\rho_w S) - 1}{\exp(\rho_w S) + 1} \tag{67}$$

where ρ_w denotes a known positive constant.

IV. SIMULATION COMPARISONS

In order to analyze the effectiveness of the proposed SFSMC, the following simulation comparisons have been accomplished in comparison with the finite-time and fixed-time sliding mode controls [12], [21], [29], [30].

A. SIMULATION COMPARISONS FOR UNCERTAIN ROBOT MANIPULATORS

To the best of our knowledge, the proposed SFSMC yields the first fixed-time sliding mode control for uncertain robot manipulators. Then, the objective of this part is to show the performance improvement of the proposed SFSMC compared with the existing finite-time sliding mode controls of uncertain robot manipulators [12], [21].

The dynamics of two-DOFs robot are given by [3]

$$M(q) = \begin{bmatrix} H_1 + 2H_2\cos(q_2) & H_3 + H_2\cos(q_2) \\ H_3 + H_2\cos(q_2) & H_4 \end{bmatrix} \tag{68}$$

$$C(q,\ \dot{q}) = \begin{bmatrix} -H_2\sin(q_2)\dot{q}_1 & -2H_2\sin(q_2)\dot{q}_1 \\ 0 & H_2\sin(q_2)\dot{q}_2 \end{bmatrix} \tag{69}$$

$$g(q) = \begin{bmatrix} H_5\cos(q_1) + H_6\cos(q_1 + q_2) \\ H_6\cos(q_1 + q_2) \end{bmatrix}^T \tag{70}$$

with

$$\begin{aligned} H_1 &= (m_1 + m_2)r_1^2 + m_2 r_2^2 + J_1, \quad H_2 = m_2 r_1 r_2 \\ H_3 &= m_2 r_2^2, \quad H_4 = H_3 + J_2 \\ H_5 &= (m_1 + m_2)r_1 g_1, \quad H_6 = m_2 r_2 g_1 \end{aligned} \tag{71}$$

The parameters of robot manipulators are summarized as follows: $J_1 = J_2 = 5.0$ kg $\cdot$ m, $m_1 = 0.5$ kg, $m_2 = 1.5$ kg,

$r_1 = 1.0$ m, $r_2 = 0.8$ m and $g_1 = 9.8$ m/s^2. The nominal value of m_1 and m_2 are $\hat{m}_1 = 0.4$ kg and $\hat{m}_2 = 1.2$ kg.

By using (68) and the given system parameters, the lower and upper bounds of the inverse inertial matrix $M(q)$ defined by (26) are given by $\gamma_1 = 0.09$ and $\gamma_2 = 0.2$, and hence $M_0 = 6.89I_n$ and $\sigma = 0.38$ given by (25) and (28), respectively. Note that $M_0(q)$ of the ITSMC [21] and the proposed SFSMC are different from the FTSMC [12], but $C_0(q,\ \dot{q})$ and $g_0(q)$ of the ITSMC [21] and the proposed SFSMC are selected in the same way as the FTSMC. In general, for the FTSMC, $M_0(q)$, $C_0(q, \dot{q})$ and $g_0(q)$ are chosen by replacing m_1 and m_2 of (68)-(71) with the nominal ones $\hat{m}_1$ and $\hat{m}_2$.

The external disturbances are

$$d = \begin{bmatrix} 2\sin(t) + 0.5\sin(200\pi t) \\ \cos(2t) + 0.5\sin(200\pi t) \end{bmatrix}^T \tag{72}$$

The desired trajectory $q_d = [q_{d1}, q_{d2}]^T$ (rad) are presented as follows

$$\begin{aligned} q_{d1} &= 1.25 - \frac{7}{5}\exp(-t) + \frac{7}{20}\exp(-4t) \\ q_{d2} &= 1.25 + \exp(-t) - \frac{1}{4}\exp(-4t) \end{aligned} \tag{73}$$

The sampling period is 1 ms. The initial conditions are defined as follows

$$q(0) = [1.0,\ 1.5]^T, \quad \dot{q}(0) = [0,\ 0]^T \tag{74}$$

Upon the above simulation conditions, the simulation comparisons are performed with the fast terminal sliding mode control (FTSMC) [12] and the integral terminal sliding mode control (ITSMC) [21] for uncertain robot manipulators. The FTSMC is given as

$$S = e + \mathrm{Sig}^{\Gamma_1}(e) + \mathrm{Sig}^{\Gamma_2}(\dot{e}) \tag{75}$$

$$\begin{aligned} \tau = -M_0(q)\Bigg[& M_2 S + (\varsigma + M_1)\frac{S}{\|S\|} + F_2 \\ & + \Gamma_2^{-1}\left(I_2 + \Gamma_1 \mathrm{D}^{\Gamma_1 - I_2}(e)\right)\mathrm{Sig}^{2I_2 - \Gamma_2}(\dot{e}) \end{aligned} \tag{76}$$

$$\varsigma = \left\| M_0^{-1}(q) \right\| \left(b_0 + b_1 \|q\| + b_2 \|\dot{q}\|^2 \right) \tag{77}$$

$$F_2 = -M_0^{-1}(q)(C(q,\ \dot{q}) + g_0(q)) - \ddot{q}_d \tag{78}$$

where M_1 and M_2 are the design positive constants, $b_i,\ i = 0,\ 1,\ 2$ denote the known positive constants, and Γ_1 and Γ_2 stand for the positive definite diagonal matrices.

A observer defined by the work [21] is given as

$$\begin{aligned} \dot{\hat{x}}_1 &= \hat{x}_2 + (\eta - w)\mathrm{sign}(e_1) \\ \dot{\hat{x}}_2 &= M_0^{-1}(\tau - C_0(q,\ \dot{q})\dot{q} - g_0(q) - M_0\ddot{q}_d) + e_2 \end{aligned} \tag{79}$$

where $x_1 = e$, $x_2 = \dot{e}$, $\hat{x}_1$ and $\hat{x}_2$ stand for the estimation of x_1 and x_2, η denotes a positive constant and

$$w = -\frac{(\gamma_1 + \gamma_2)}{2}\sqrt{n}(a_0 + a_1\|\dot{q}\|^2 + \sigma\|\tau\|) \tag{80}$$

where γ_1, γ_2, a_1, a_2 and σ are defined as (26) and (29), respectively, and the integral terminal sliding mode

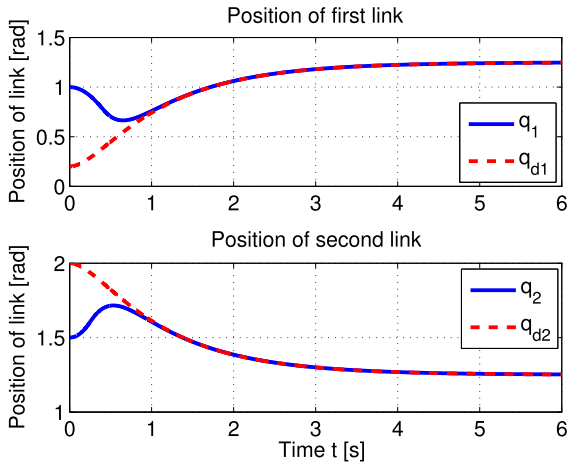

FIGURE 3. Position of joints of SFSMC.

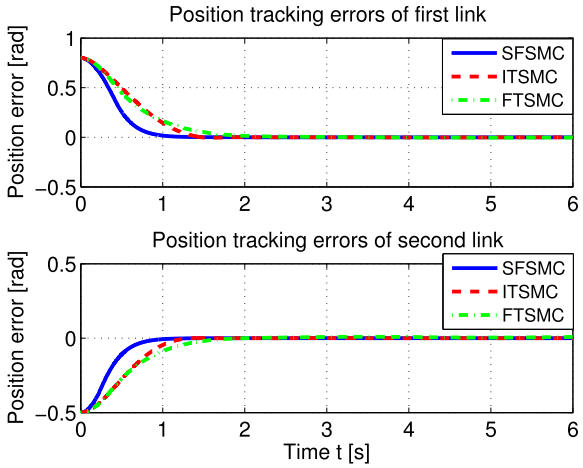

FIGURE 4. Position tracking error of SFSMC, ITSMC and FTSMC.

control (ITSMC) [21] are

$$\hat{S} = \hat{x}_2 + \int_0^t \left[K_p \mathrm{Sig}^{\alpha_1}(x_1(\sigma)) + K_d \mathrm{Sig}^{\alpha_2}(x_2(\sigma))\right]\mathrm{d}\sigma \tag{81}$$

$$\tau = \tau_1 + \tau_2 \tag{82}$$

$$\tau_1 = C_0(q,\ \dot{q})\dot{q} + g_0(q) + M_0\ddot{q}_d \tag{83}$$

$$\begin{aligned} \tau_2 = & -M_0\left[K_p \mathrm{Sig}^{\alpha_1}(x_1) + K_d \mathrm{Sig}^{\alpha_2}(x_2)\right] \\ & -M_0\left[\lambda_1 \mathrm{Sig}^{1/2}(\hat{S}) + \int_0^t \lambda_2 \mathrm{sign}(\hat{S})d\sigma\right] \end{aligned} \tag{84}$$

where K_p and K_d are two positive definite diagonal matrices, $\alpha_2 = 2\alpha_1/(\alpha_1 + 1)$ with $0 < \alpha_1 < 1$, and λ_1 and λ_2 are two design positives.

Remark 4: For a fair comparison, the parameters of the FTSMC and ITSMC are the same as the work [12], [21]. For the proposed SFSMC, the parameters are selected by trailing the position tracking error until an improved performance is obtained without using excessive control input. They are listed in Table 1.

Figure 3 depicts the better tracking performance of SFSMC. The position tracking errors, zoomed position tracking errors and the requested input torques are shown in Figures 4-6, respectively. Observed by Figure 4, these three

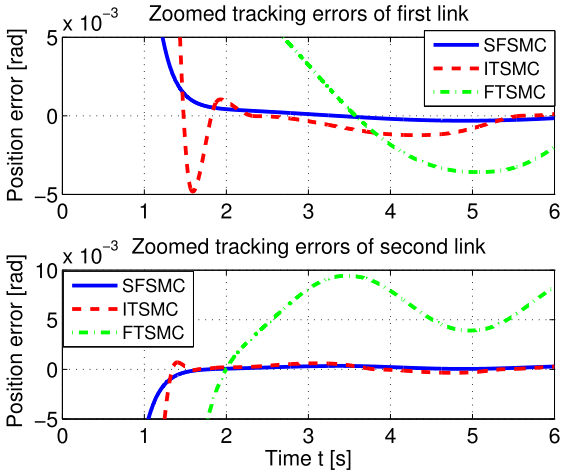

FIGURE 5. Zoomed position tracking errors of SFSMC, ITSMC and FTSMC.

TABLE 1. The parameters of SFSMC, ITSMC and FTSMC.

Controllers	Parameters
SFSMC	$\delta = 0.3,\ \alpha = 0.7,\ r = 1.7$ $\beta = 1.9,\ C_1 = 3I_2,\ C_2 = 3I_2$ $K_1 = K_2 = 5I_2,\ \nu_1 = 2.5$ $\nu_2 = 0.5,\ a_0 = 12,\ a_1 = 2.2$
ITSMC [21]	$a_0 = 12,\ a_1 = 2.8,\ \eta = 2$ $K_p = 7I_2,\ K_d = 5I_2$ $\alpha_1 = 0.5,\ \lambda_1 = \lambda_2 = 2$
FTSMC [12]	$\Gamma_1 = \mathrm{diag}\{2, 2\},\ M_1 = M_2 = 2$ $\Gamma_2 = \mathrm{diag}\{5/3, 5/3\},\ b_0 = 12$ $b_1 = 2.2, b_2 = 2.8$

controllers ensure that the trajectory of system states track the desired trajectories completely after a transient. Moreover, the proposed SFSMC without using the excessive control inputs obtains faster transient and higher steady-state tracking precision in comparison with the FTSMC and ITSMC from Figures 4-6. By using the approximation of discontinuous function (67) instead of the boundary layer to avoid the chattering, in addition, it is clear that the proposed SFSMC obtains higher steady-state precision than the FTSMC and ITSMC from Figure 5.

In order to show the advantages of the proposed SFSMC, the tracking errors plot of the proposed SFSMC with the same parameters given by Table 1 and three different initial states has been accomplished in Figure 7. These three different initial states are as follows

$$\begin{aligned}
&\text{Case 1}: \ q(0) = [1.0,\ 1.5]^T, \quad \dot{q}(0) = [0,\ 0]^T \\
&\text{Case 2}: \ q(0) = [1.5,\ 0.5]^T, \quad \dot{q}(0) = [0,\ 0]^T \\
&\text{Case 3}: \ q(0) = [-0.5,\ 3.5]^T, \quad \dot{q}(0) = [0,\ 0]^T
\end{aligned} \tag{85}$$

According to the reaching and sliding time given by (47) and (48), without any retuning of the control parameters, the settling time is bounded by a constant $T_{\max} = 4.21$ s. Observed by Figure 7, the settling time of the proposed SFSMC with three different initial states are upper bounded by 2 s, which further verifies the upper-bound estimation in Theorem 1 (i.e., $T < T_{\max} = 4.21$ s). In comparison with the settling time of the finite-time sliding mode controls (see (4), (10) and (13) of [12] and (11) and (40) of [21]), in addition, the upper bound of the convergence time of the proposed SFSMC given by (47) and (48) is a known constant ($T_{\max} = 4.21$ s) regardless of the initial states and robot model.

In order to show the effect of control parameters on the tracking performance of the proposed SFSMC, the tracking errors plot in sliding phase ($S = 0$ according to (6), (8), (30), (34) and (36)) with three sets of parameters has been accomplished in Figure 8. These three sets of parameters are

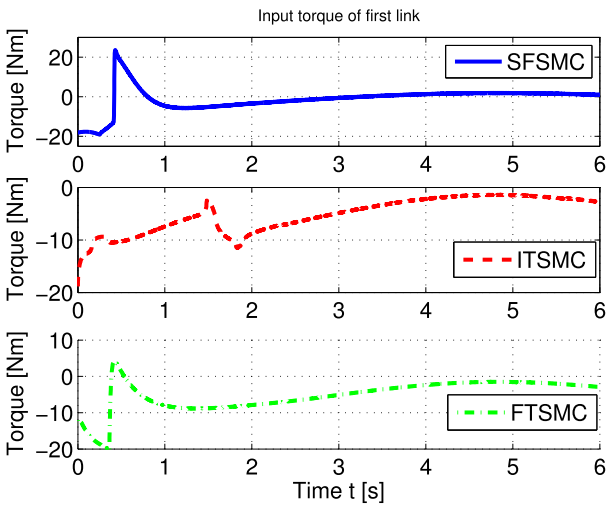

(a) The input torque of first link.

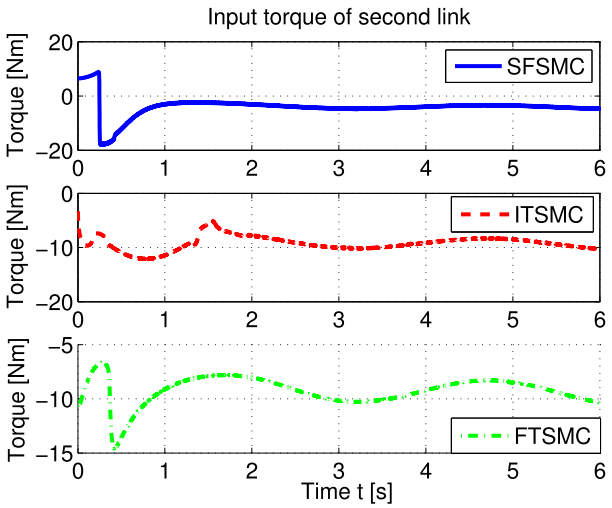

(b) The input torque of second link.

FIGURE 6. Requested inputs of SFSMC, ITSMC and FTSMC.

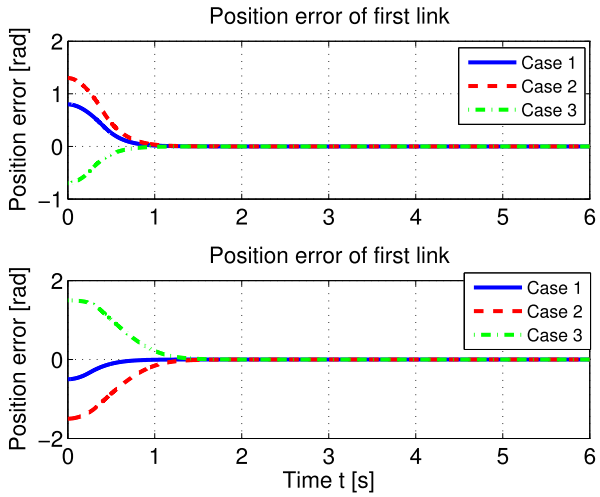

FIGURE 7. Position tracking errors of SFSMC with three different initial states.

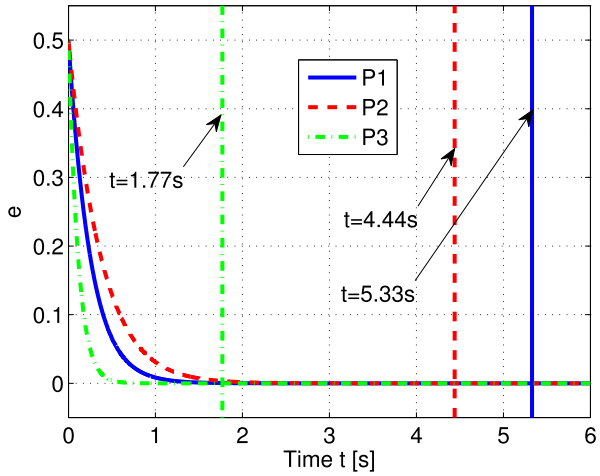

FIGURE 8. Convergence of SFSMC with different parameters.

as follows

$$\begin{aligned} &\text{P1}: \alpha = 0.7, \quad \delta = 0.3, \ \beta = 1.5, \ C_1 = C_2 = 2 \\ &\text{P2}: \alpha = 0.7, \quad \delta = 0.3, \ \beta = 1.9, \ C_1 = C_2 = 2 \\ &\text{P3}: \alpha = 0.7, \quad \delta = 0.3, \ \beta = 1.9, \ C_1 = C_2 = 5 \end{aligned} \tag{86}$$

According to the sliding time (48), with retuning of the control parameters, the settling time of P1, P2 and P3 is bounded by different constants (according to (48), P1 : $T_{\max} = 5.33$ s; P2 : $T_{\max} = 4.44$ s; P3 : $T_{\max} = 1.77$ s;). Observed by Figure 8, the proposed SFSMC with three sets of parameters have different upper bounds which are always bounded by their upper bound of the settling time regardless of the initial states (i.e., P1 : $T < T_{\max} = 5.33$ s; P2 : $T < T_{\max} = 4.44$ s; P3 : $T < T_{\max} = 1.77$ s;). The simulation comparisons in Figure 8 further verifies the upper-bound estimation in Theorem 1 (i.e. $T < T_{\max}$). Obviously, the gains C_1 and C_2 have more influence on the tracking performance than the β. However, the control input

TABLE 2. Comparison of control performance.

Controllers	$\|e\|_{\text{IAE}}$	$\|\tau\|_{\text{ECI}}$
SFSMC	3.1463×10^{-4}	9.1150
ITSMC [21]	4.2653×10^{-4}	9.7362
FTSMC [12]	6.2688×10^{-4}	9.6456

will be increased with the increasing gains C_1 and C_2. Thus, the parameters selection of our paper is a balance between the tracking performance and the control input torque.

To further quantize the steady-state tracking performance of the proposed SFSMC, the following integrated absolute error (IAE) and energy of control input (ECI) [35] are compared after 2 seconds at the beginning of simulation comparisons.

$$\|e\|_{\text{IAE}} = \sqrt{\frac{1}{N}\sum_{k=1}^{N}\|e(k)\|^2} \tag{87}$$

$$\|\tau\|_{\text{ECI}} = \sqrt{\frac{1}{N}\sum_{k=1}^{N}\|\tau(k)\|^2} \tag{88}$$

where N is the total number of samples, and $e(k)$ and $\tau(k)$ stand for the position tracking error and the control input of joint at the $k-$th sampling instant, respectively. The comparisons of two performance indexes are summarized in Table 2.

As shown in Table 2, the proposed SFSMC without using an excessive ECI can obtain the minimal IAE than the FTSMC and ITSMC. The comparison results of Table 2 are to further verify the performance improvement of the proposed SFSMC in comparison with the existing finite-time sliding mode controls for uncertain robot manipulators [12], [21].

B. SIMULATION COMPARISONS FOR SIP SYSTEM

For the existing fixed-time sliding mode controls (FSMC) [29], [30], the exact control gain has been required in the formulation of the fixed-time sliding mode control. It means that these FSMCs cannot directly adopted for uncertain robot manipulators (see Remark 2). Then, in order to obtain a fair simulation comparisons, numerical comparisons have been accomplished for the single inverted pendulum (SIP) system in comparison with these FSMCs [29], [30].

First, consider the following SIP system

$$\begin{cases} \dot{x}_1 = x_2 \\ \dot{x}_2 = f + bu + d \end{cases} \tag{89}$$

where

$$\begin{aligned} f &= \frac{g_1 \sin(x_1) - mlx_2^2 \cos(x_1)\sin(x_1)/(m_c+m)}{l[4/3 - m\cos^2(x_1)/(m_c+m)]} \\ b &= \frac{\cos(x_1)/(m_c+m)}{l[4/3 - m\cos^2(x_1)/(m_c+m)]} \end{aligned} \tag{90}$$

where x_1 and x_2 denote the angular position and velocity of the pole, respectively, u stands for the applied force and d denotes the external disturbance.

The parameters of SIP system are summarized as follows: $m_c = 1$ kg, $m = 0.1$ kg, $l = 0.5$ m and $g_1 = 9.8$ m/s^2. The sampling period is 1 ms. The initial states are set as $x_1(0) = 1$ and $x_2(0) = 0.5$. The desired trajectories x_{1d} and the external disturbance d are given as

$$x_{1d} = \sin(0.5\pi t), \quad d = \sin(10x_1) + \cos(x_2) \tag{91}$$

The tracking errors denoted by $e_1,\ e_2 \in R$ are defined as

$$e_1 = x_1 - x_{1d}, \quad e_2 = x_2 - x_{2d} \tag{92}$$

Accordingly, the dynamics equation for e_1 and e_2 can be given as

$$\begin{cases} \dot{e}_1 = e_2 \\ \dot{e}_2 = f - \ddot{x}_{1d} + bu + d \end{cases} \tag{93}$$

According to (30), (36) and (40)-(44), the proposed SFSMC for the SIP system is derived as

$$S = e_2 + C_1 f(e_1) + C_2 \mathrm{sig}^{\beta}(e_1) \tag{94}$$

$$\begin{aligned} u = -b^{-1}\Big[&f - \ddot{x}_{1d} + C_1 h(e_1)e_2 + C_2\beta|e_1|^{\beta-1}e_2 \\ &+ k\psi(\rho,\ S) + a_3\mathrm{sig}^{\gamma_1}(S) + c_3\mathrm{sig}^{\gamma_2}(S)\Big] \end{aligned} \tag{95}$$

where $\mathrm{sign}(\cdot), f(\cdot), h(\cdot)$ and $\psi(\rho,\ S)$ are defined by (8), (30), (32) and (67), respectively.

The comparisons are performed with the fast fixed-time sliding mode control (FFSMC) [30] and the non-singular fixed-time sliding mode control (NFSMC) [29]. The FFSMC is [30]

$$S = \mathrm{sig}^{a_1}(e_1) + \frac{k_2 a_2}{2a_2 - 1}\mathrm{sig}^{2-1/a_2}(e_2 + k_1\mathrm{sig}^{a_1}(e_1)) \tag{96}$$

$$\begin{aligned} u = -b^{-1}\Big[&f - \ddot{x}_{1d} + k_1 a_1 |e_1|^{a_1-1}\left(\frac{\phi}{k_1} + e_2\right) \\ &+ a\mathrm{sig}^{\gamma_1}(S) + c\mathrm{sig}^{\gamma_2}(S) + k\psi(\rho,\ S)\Big] \end{aligned} \tag{97}$$

where $k_1 > 0, k_2 > 0, k > 0, a_2 > 1, 1 < a_1 < 2 - 1/a_2$, $\gamma_1 > 1, 0 < \gamma_2 < 1$, $\psi(\rho,\ S)$ is defined by (67) and

$$\phi = \frac{1}{k_2}\mathrm{sig}^{1/a_2}(e_2 + k_1\mathrm{sig}^{a_1}(e_1)) + \frac{k_1 a_2}{2a_2 - 1}(e_2 + k_1\mathrm{sig}^{a_1}(e_1)) \tag{98}$$

The NFSMC for SIP is given as [29]

$$S = e_1 + \mathrm{sig}^{q_1/p_1}(\kappa e_1) \tag{99}$$

$$\begin{aligned} u = -b^{-1}\Big[&f - \ddot{x}_{1d} + \gamma\,\mathrm{sign}(S) \\ &+ \frac{p_1}{q_1}\kappa^{-\frac{q_1}{p_1}}\mu_\tau|e_2|^{1-\frac{q_1}{p_1}}\left(a_2\mathrm{sig}^{\frac{m_2}{n_2}}(S) + c_2\mathrm{sig}^{\frac{p_2}{q_2}}(S)\right)\Big] \\ &+ \frac{1}{b\kappa}\Big[a_1\left(\frac{m_1}{n_1} - \frac{p_1}{q_1}\right)\mathrm{sig}^{m_1/n_1 - p_1/q_1 - 1}(e_1)\kappa^2 e_2^2 \\ &- \frac{p_1}{q_1}\kappa^{1-q_1/p_1}\mathrm{sig}^{2-q_1/p_1}(e_2)\Big] \end{aligned} \tag{100}$$

where

$$\kappa(e_1) = \frac{1}{a_1|e_1|^{m_1/n_1 - p_1/q_1} + c_1} > 0 \tag{101}$$

$$\mu_\tau = \begin{cases} \sin\left(\frac{\pi}{2}\frac{|e_2|^{q_1/p_1 - 1}}{\vartheta_1}\right), & \text{if } |e_2|^{q_1/p_1 - 1} \le \vartheta_1 \\ 1, & \text{otherwise} \end{cases} \tag{102}$$

TABLE 3. The parameters of SFSMC, FFSMC and NFSMC.

Controllers	Parameters
SFSMC	$\delta = 0.2,\ \alpha = 0.8,\ r = 1.8,\ \beta = 1.1$ $C_1 = 5,\ C_2 = 1.5,\ a_3 = 3$ $c_3 = 5,\ \gamma_1 = 1.1,\ \gamma_2 = 0.8$
FFSMC [30]	$k_1 = 5,\ k_2 = 0.1,\ a_1 = 1.1$ $a_2 = 3,\ a = c = 1,\ \gamma_1 = 5/3$ $\gamma_2 = 5/9,\ k = 2,\ \rho = 100$
NFSMC [29]	$a_1 = c_1 = 2,\ a_2 = c_2 = 1,\ m_1 = 9$ $n_1 = 5,\ p_1 = 7,\ q_1 = 9,\ m_2 = 5$ $n_2 = 3,\ p_2 = 5,\ q_2 = 9,\ \tau_1 = 0.1$

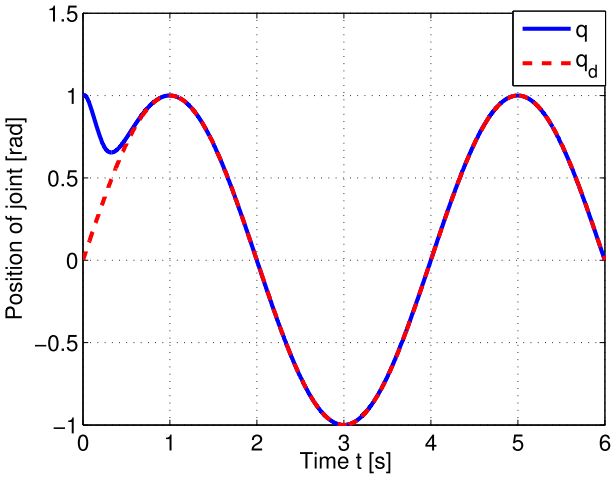

FIGURE 9. Position of joints of SFSMC.

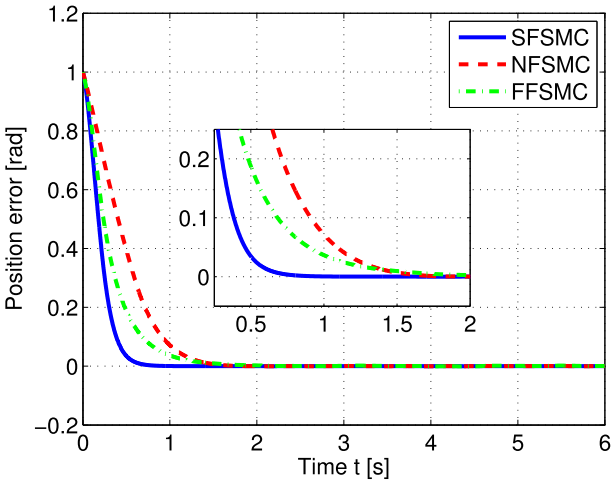

FIGURE 10. Position tracking errors of SFSMC, NFSMC and FFSMC.

The parameters of the FFSMC and NFSMC are the same as the work [29], [30]. For the proposed SFSMC, the parameters are selected by trailing the position tracking error until an improved performance is obtained without using excessive control input. They are listed in Table 3.

Figure 9 depicts the better tracking performance of the proposed SFSMC for the SIP system. The position tracking errors, zoomed position tracking errors and the requested input torques are shown in Figures 10-12, respectively.

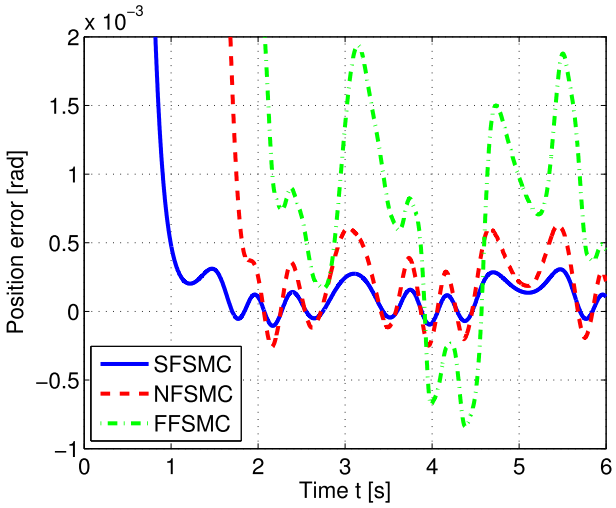

FIGURE 11. Zoomed position tracking errors of SFSMC, NFSMC and FFSMC.

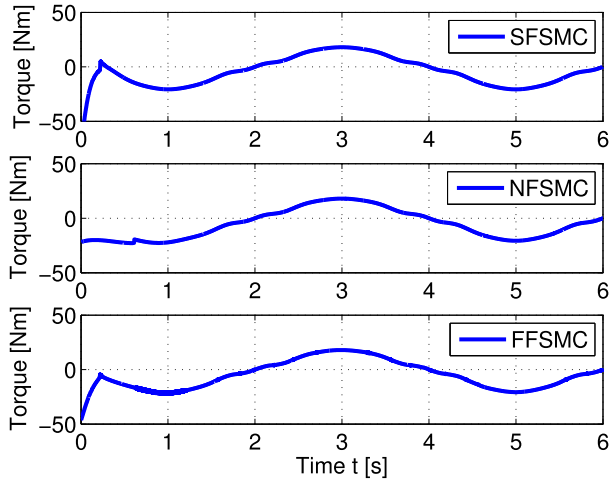

FIGURE 12. Requested input of SFSMC, NFSMC and FFSMC.

TABLE 4. Comparison of control performance.

Controllers	$\|e\|_{\mathrm{IAE}}$	$\|\tau\|_{\mathrm{ECI}}$
SFSMC	1.174×10^{-4}	9.0844
FFSMC [30]	7.4912×10^{-4}	9.0837
NFSMC [29]	2.3818×10^{-4}	9.0852

Observed by Figure 10, these three controllers ensure that the trajectory of the system states track the desired trajectories completely after a transient. We can conclude from Figures 10-12 that the proposed SFSMC also shows the improved tracking performance such as faster transient and higher steady-state tracking precision for SIP system over the existing fixed-time sliding mode controls [29], [30] with the exact control gain b.

Similar to (87) and (88), these two performance indexes are summarized in Table 4 to further quantize the steady-state tracking performance of the proposed SFSMC, FFSMC and NFSMC for SIP system.

As shown in Table 4, the proposed SFSMC without using an excessive ECI can obtain the minimal IAE than the

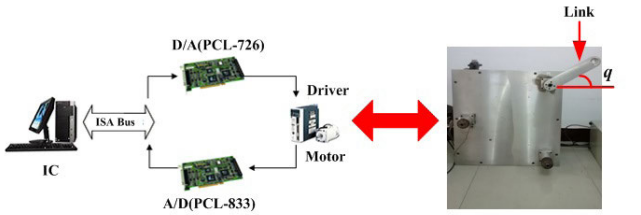

FIGURE 13. The experimental robot setup.

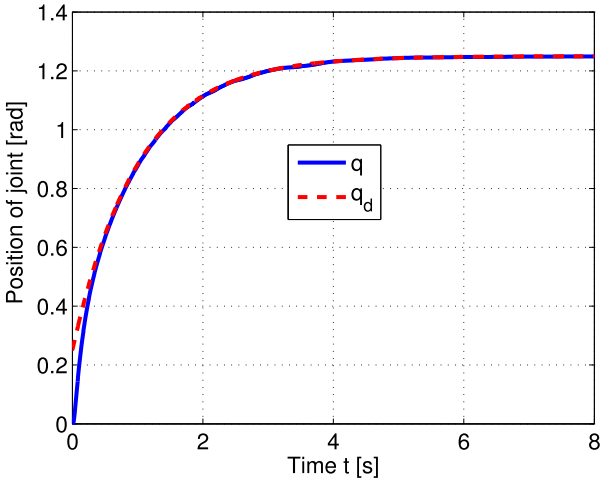

FIGURE 14. Position of joint by using SFSMC.

FFSMC and NFSMC. The comparison results of Table 4 are to further verify the improved tracking performance of the proposed SFSMC for SIP system over the fixed-time sliding mode controls [29], [30].

Upon the basis of the above simulation comparisons in Sections **A** and **B**, whether the exact control gain b is known or not, the proposed SFSMC always achieves the improved performance such as faster transient and higher steady-state tracking precision than the existing finite-time and fixed-time sliding mode controls [12], [21], [29], [30].

V. EXPERIMENTAL RESULTS

In this section, the effectiveness of the proposed controller are further validated with experiments on a one-DOF mechanical system as shown in Figure 13. The link of the one-DOF mechanical system is driven by an AC motor with the associated driver. The position of link is obtained from a 17 bit absolute encoder. This position information is transmitted into an Advantech industrial computer (IC) by the interface board PCL-833. The control torque is transmitted into the motor through the board PCL-726. The program is written with Microsoft Visual C++ 6.0.

The gravity torque of the robot is $g\,(q) = 1.14\cos(q)$ (Nm). The sampling period is $T = 2$ ms. The desired trajectory is $q_{d1} = 1.25 - 7/5\exp(-t) + 7/20\exp(-4t)$ (rad). The initial states are selected as zero. For a fair comparison, in this section, the parameters of the SFSMC, ITSMC and FTSMC

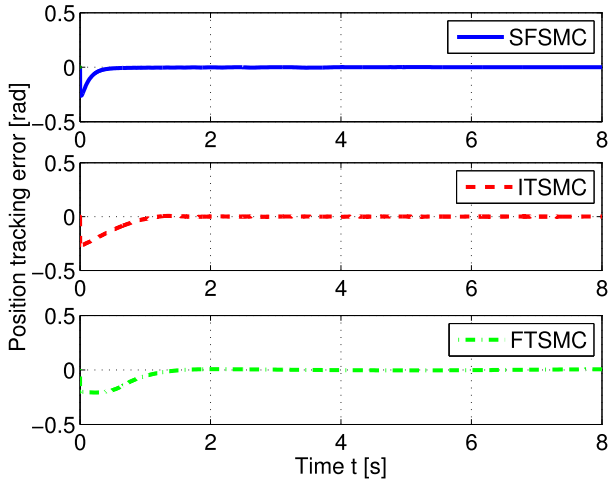

FIGURE 15. Experimental position tracking errors.

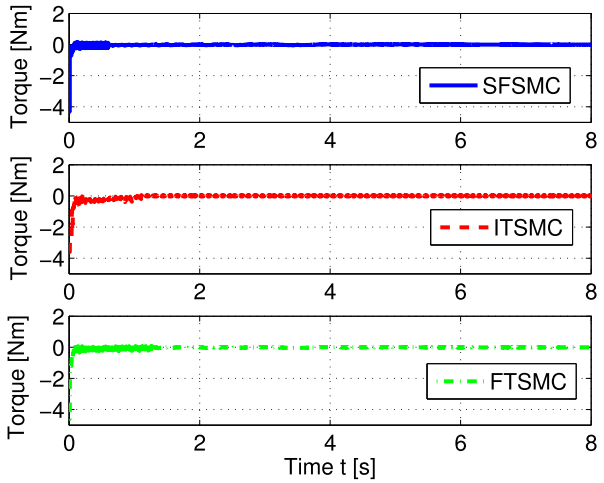

FIGURE 16. Experimental control torque.

will be selected by trailing the ECI of control input until faster transient and higher steady-state tracking precision are obtained without using the excessive ECI. The parameters of the proposed SFSMC are $\alpha = 0.7, \delta = 0.3, r = 1.7, \beta = 1.9$, $\beta_2 = 0.5, a_0 = 12, a_1 = 2.2, \nu_1 = 1.1, \nu_2 = 0.5, a_0 = 12$, $a_1 = 2.2, C_1 = 5, C_2 = 1$, and $K_1 = K_2 = 4$. The parameters of the FTSMC are $\Gamma_1 = 1.5, \Gamma_2 = 1.4, M_1 = 1, M_2 = 1$, $b_0 = 20, b_1 = 12$, and $b_2 = 2.8$; while the parameters of the ITSMC are $\lambda_1 = \lambda_2 = 1, \alpha_1 = 0.5, b_0 = 12, b_2 = 2.8$ and $K_p = K_d = 4$.

Figure 14 depicts the improved tracking performance of the proposed SFSMC for one-DOF mechanical system. Figures 15 and 16 show the position tracking errors and the requested inputs of the SFSMC, FTSMC and ITSMC, respectively. Obviously, from Figures 15 and 16, the experimental results further verify that the proposed controller achieves an improved tracking performance such as faster transient and smaller steady-state tracking error without using an excessive control input.

TABLE 5. Comparison of control performance.

Controllers	$\|e\|_{\mathrm{IAE}}$	$\|\tau\|_{\mathrm{ECI}}$
SFSMC	1.36×10^{-3}	0.013
FTSMC [12]	3.6×10^{-3}	0.031
ITSMC [21]	6.8×10^{-3}	0.018

Similarly, we use IAE and ECI defined by (87) and (88) to quantize the improved performance of the proposed SFSMC than that of FTSMC and ITSMC. These two performance indexes defined by (87) and (88) are compared after 2 seconds at the beginning of the experimental comparisons. The comparisons of these two performance indexes are summarized in Table 5.

As shown in Table 5, the proposed SFSMC without using an excessive ECI can obtain the minimal IAE than the ITSMC [21] and FTSMC [12]. According to the experimental results, the position error of the proposed SFSMC takes lesser convergence time than the ITSMC and FTSMC. The comparison described by Table 5 further verifies the improved tracking performance of the proposed SFSMC.

VI. CONCLUSION

In this paper, a novel singularity-free fixed-time sliding mode control have been developed for global fixed-time tracking of robot manipulators subject to uncertain dynamics and bounded external disturbances. Advantages of the proposed approach includes the elimination of singularity completely and having an ability for the convergence of both sliding surface and tracking errors within a fixed time. The proposed control ensures that the total settling time of the robot system is independent of the initial states and can be estimated in advance. In comparison with the existing fixed-time sliding mode controls [29], [30], the proposed SFSMC can be used for multi-DOFs robot system directly. The developed approach offers an alternative to improve the fixed-time tracking performance of uncertain robot manipulators. The future work includes the development of the proposed SFSMC to the velocity-free fixed-time sliding mode control.

REFERENCES

[1] Z. H. Man, A. P. Paplinski, and H. R. Wu, "A robust MIMO terminal sliding mode control scheme for rigid robotic manipulators," *IEEE Trans. Autom. Control*, vol. 13, no. 1, pp. 11–23, Dec. 1994.
[2] Y. Tang, "Terminal sliding mode control for rigid robots," *Automatica*, vol. 34, no. 1, pp. 51–56, 1998.
[3] Y. Feng, X. Yu, and Z. Man, "Non-singular terminal sliding mode control of rigid manipulators," *Automatica*, vol. 38, no. 12, pp. 2159–2167, 2002.
[4] S. Yu, X. Yu, B. Shirinzadeh, and Z. Man, "Continuous finite-time control for robotic manipulators with terminal sliding mode," *Automatica*, vol. 41, no. 11, pp. 1957–1964, Nov. 2005.
[5] J. Baek, W. Kwon, B. Kim, and S. Han, "A widely adaptive time-delayed control and its application to robot manipulators," *IEEE Trans. Ind. Electron.*, vol. 66, no. 7, pp. 5332–5342, Jul. 2019.
[6] A. T. Vo and H.-J. Kang, "A chattering-free, adaptive, robust tracking control scheme for nonlinear systems with uncertain dynamics," *IEEE Access*, vol. 7, pp. 10457–10466, 2019.
[7] Q. Yan, J. Cai, Y. Ma, and Y. Yu, "Robust learning control for robot manipulators with random initial errors and iteration-varying reference trajectories," *IEEE Access*, vol. 7, pp. 32628–32643, 2019.

[8] S. Baek, J. Baek, and S. Han, "An adaptive sliding mode control with effective switching gain tuning near the sliding surface," *IEEE Access*, vol. 7, pp. 15563–15572, 2019.
[9] Z. Chen, X. Yang, X. Zhang, and P. X. Liu, "Finite-time trajectory tracking control for rigid 3-DOF manipulators with disturbances," *IEEE Access*, vol. 6, pp. 45974–45982, 2018.
[10] S. T. Venkataraman and S. Gulati, "Control of nonlinear systems using terminal sliding modes," *J. Dyn. Syst., Meas., Control*, vol. 115, no. 3, pp. 554–560, 1993.
[11] K.-B. Park and J.-J. Lee, "Comments on 'a robust MIMO terminal sliding mode control scheme for rigid robotic manipulators,'" *IEEE Trans. Autom. Control*, vol. 41, no. 5, pp. 761–762, May 1996.
[12] L. Yang and J. Yang, "Nonsingular fast terminal sliding-mode control for nonlinear dynamical systems," *Int. J. Robust Nonlinear Control*, vol. 21, no. 16, pp. 1865–1879, 2011.
[13] M. Jin, J. Lee, P. H. Chang, and C. Choi, "Practical nonsingular terminal sliding-mode control of robot manipulators for high-accuracy tracking control," *IEEE Trans. Ind. Electron.*, vol. 56, no. 9, pp. 3593–3601, Sep. 2009.
[14] M. Galicki, "Finite-time control of robotic manipulators," *Automatica*, vol. 51, pp. 49–54, Jan. 2015.
[15] M. Galicki, "Finite-time trajectory tracking control in a task space of robotic manipulators," *Automatica*, vol. 67, pp. 165–170, May 2016.
[16] W.-H. Zhu, "Comments on 'robust tracking control for rigid robotic manipulators,'" *IEEE Trans. Autom. Control*, vol. 45, no. 8, pp. 1577–1580, Aug. 2000.
[17] B. Xian, D. M. Dawson, M. S. D. Queiroz, and J. Chen, "A continuous asymptotic tracking control strategy for uncertain nonlinear systems," *IEEE Trans. Autom. Control*, vol. 49, no. 7, pp. 1206–1211, Jul. 2004.
[18] O. Barambones and V. Etxebarria, "Energy-based approach to sliding composite adaptive control for rigid robots with finite error convergence time," *Int. J. Control*, vol. 75, no. 5, pp. 352–359, 2002.
[19] D. Zhao, S. Li, and F. Gao, "A new terminal sliding mode control for robotic manipulators," *Int. J. Control*, vol. 82, no. 10, pp. 1804–1813, 2009.
[20] L. Wang, T. Chai, and L. Zhai, "Neural-network-based terminal sliding mode control of robotic manipulators including actuator dynamics," *IEEE Trans. Ind. Electron.*, vol. 56, no. 9, pp. 3296–3304, Sep. 2009.
[21] L. Zhang, L. Liu, Z. Wang, and Y. Xia, "Continuous finite-time control for uncertain robot manipulators with integral sliding mode," *IET Control Theory Appl.*, vol. 12, no. 11, pp. 1621–1627, Jul. 2018.
[22] V. Andrieu, L. Praly, and A. Astolfi, "Homogeneous approximation, recursive observer design, and output feedback," *SIAM J Control Optim.*, vol. 47, no. 4, pp. 1814–1850, 2009.
[23] A. Polyakov, "Nonlinear feedback design for fixed-time stabilization of linear control systems," *IEEE Trans. Autom. Control*, vol. 57, no. 8, pp. 2106–2110, Aug. 2012.
[24] A. Polyakov, D. Efimov, and W. Perruquetti, "Robust stabilization of MIMO systems in finite/fixed time," *Int. J. Robust Nonlinear Control*, vol. 26, no. 1, pp. 69–90, 2016.
[25] A. Levant, "On fixed and finite time stability in sliding mode control," in *Proc. IEEE Conf. Decis. Control*, Florence, Italy, Dec. 2013, pp. 4260–4265.
[26] B. Tian, Z. Zuo, X. Yan, and H. Wang, "A fixed-time output feedback control scheme for double integrator systems," *Automatica*, vol. 80, pp. 17–24, Jun. 2017.
[27] E. Jiménez-Rodríguez, J. D. Sánchez-Torres, and A. G. Loukianov, "On optimal predefined-time stabilization," *Int. J. Robust Nonlinear Control*, vol. 27, no. 17, pp. 3620–3642, Nov. 2017.
[28] Z. Zuo, "Nonsingular fixed-time consensus tracking for second-order multi-agent networks," *Automatica*, vol. 54, pp. 305–309, Apr. 2015.
[29] Z. Zuo, "Non-singular fixed-time terminal sliding mode control of nonlinear systems," *IET Control Theory Appl.*, vol. 9, no. 4, pp. 545–552, Feb. 2014.
[30] H. Li and Y. Cai, "On SFTSM control with fixed-time convergence," *IET Control Theory Appl.*, vol. 11, no. 6, pp. 766–773, Apr. 2017.
[31] L. Sciavicco and B. Siciliano, *Modelling and Control of Robot Manipulators*. London, U.K.: Springer-Verlag, 2012.
[32] Z. Zuo and L. Tie, "Distributed robust finite-time nonlinear consensus protocols for multi-agent systems," *Int. J. Syst. Sci.*, vol. 47, no. 6, pp. 1366–1375, Apr. 2016.
[33] L. Zhang, Y. Su, and Z. Wang, "A simple non-singular terminal sliding mode control for uncertain robot manipulators," *Proc. Inst. Mech. Eng., I, J. Syst. Control Eng.*, vol. 233, no. 6, pp. 666–676, Jul. 2019.
[34] H. K. Khalil, *Nonlinear Systems*, 3rd ed. Upper Saddle River, NJ, USA: Prentice-Hall, 2005.
[35] S. Skogestad, "Simple analytic rules for model reduction and PID controller tuning," *J. Process Control*, vol. 13, no. 4, pp. 291–309, Jun. 2003.

LIYIN ZHANG received the B.S. degree in communication engineering from Ningxia University, Ningxia, China, in 2008, the M.S. degree in circuits and systems from Xidian University, Xi'an, China, in 2014, and the Ph.D. degree in mechanical manufacture and automation from Xidian University, Xi'an, in 2018. He is currently a Lecturer with the School of Automation, Xi'an University of Posts and Telecommunications. His current interests include the sliding mode control, feedback control, and fault-tolerant control for nonlinear system with matched and mismatched disturbances.

YOUMING WANG received the M.S. and Ph.D. degrees in mechanical engineering from the Xi'an University of Technology and Xi'an Jiaotong University, Xi'an, China, in 2006 and 2010, respectively. He is currently a Professor with the Xi'an University of Posts and Telecommunications. His current interests include fault diagnosis, vibration control, and structural health management.

YINLONG HOU received the M.S. and Ph.D. degrees in instrument science and technology from the Beijing Institute of Technology, China, in 2013 and 2018, respectively. He is currently a Lecturer with the School of Automation, Xi'an University of Posts and Telecommunications. His research interests include optical measurement, adaptive optics, and intelligent control.

HONG LI received the B.S. degree in electronic information engineering from Chongqing Communication University, Chongqing, China, in 2008, the M.S. degree in signal and information processing from Xi'an Technological University, Xi'an, China, in 2012, and the Ph.D. degree in navigation and control from Northwestern Polytechnical University, Xi'an, China, in 2018. She is currently a Lecturer with the School of Automation, Xi'an University of Posts and Telecommunications. Her research interests include artificial intelligence and intelligent optimization algorithms.